EMI CHARACTERISTICS OF A POTENTIAL CONTROL SYSTEM*

D. E. Donatelli
Boston College
Chestnut Hill, Massachusetts 02167

H. A. Cohen and W. J. Burke
Air Force Geophysics Laboratory
Hanscom Air Force Base, Massachusetts 01731

H. C. Koons
The Aerospace Corporation
Los Angeles, California 90009

With the development and use of charged particle sources for controlling space-craft potentials there is a need to better understand the effects of these systems on spacecraft operations. The emission of charged particles perturbs the spacecraft environment and signals are generated which may interfere with other vehicle functions. In particular, the generated signals are apt to interfere with detectors for observing waves that exist naturally in the space environment. Examples of this type of inter-ference are presented from the SCATHA satellite during a period when the vehicle was highly charged. A plasma source on board the spacecraft succeeded in discharging the vehicle with each of four different operating modes. The VLF broadband receiver on SCATHA detected interference over the entire 0-5 kHz range of both the electric and magnetic field detectors during these charged particle emissions. This frequency range includes the 2 kHz electron gyrofrequency but is below the 9 kHz electron plasma frequency. The observations suggest that interference occurs through introduction of anomalous signals, and through suppression of background field measurements.

INTRODUCTION

The development of active means for controlling spacecraft potentials is moti-vated from both engineering and scientific considerations. Large spacecraft potentials may be responsible for operational anomalies (ref. 1 and references therein) and may interfere with measurements of the characteristics of the cold plasma embedded in the plasma sheet. The cold plasma plays a significant role in providing neutralizing currents to spacecraft (ref. 1). It also acts as a catalyst for the generation of wave turbulence in the plasma sheet (ref. 2 and 3). The waves cause energetic electrons to diffuse in pitch angle (ref.4 and 5). The lifetime of the charging environment should then be controlled by the diffusion rate of these electrons. Thus, exact measurements of the low density, cold plasma component in the plasma sheet is required both for specifying severe charging environments and for modelling their dynamics. Unfortunately, the densities and temperatures of the cold electron and ion populations can only be measured if the satellite potential is maintained at low values relative to the plasma.

Charge ejection systems have been proposed for satellite missions to facilitate measurement of cold plasma fluxes by actively maintaining the entire satellite close to plasma potential. Purvis and Bartlett (ref. 6) have pointed out that during a 92-hour period of continuous charged particle ejection by ATS-6, no spacecraft charging events were detected, although several plasma injection events were encountered. Experience with similiar injection events suggests that if the charge ejection system had not been operating, severe charging would have occurred.

Electron beam and plasma beam systems were put on the SCATHA satellite to study the discharging of satellites near geostationary orbit. During the satellite-eclipse period of 24 April 1979, SCATHA encountered such an environment and satellite potentials as low as -8 kV were measured (ref. 7). Attempts were made to discharge the vehicle using both beam systems. The electron beam system was able to raise the vehicle potential to -1 kV, but not bring about complete discharge. During periods of plasma-beam emissions the vehicle was completely discharged.

Few, if any, direct measurements of electromagnetic interference (EMI) generated during plasma beam operations have been published in the technical literature. The purpose of this report is to consider the impact of EMI generated by the emitted plasma on the operation of wave experiments. Since SCATHA is equipped with a plasma beam system and a VLF experiment capable of monitoring beam-induced waves, it provides a unique set of measurements for an EMI impact assessment. Even though there are major differences between the plasma-beam system flown on SCATHA and the charge ejection systems proposed for vehicle potential control, these measurements should have relevance for a satellite that will spend a significant fraction of its life in plasma sheet environments similiar to those encountered by SCATHA.

In the following section the plasma beam and VLF instruments on SCATHA are described. The observations section examines VLF measurements taken during the eclipse period of 24 April (day 114) 1979. In a fifteen-minute period of intermittent plasma-bea emissions, four different modes of plasma emissions successfully discharged the vehicle.

INSTRUMENTATION

SCATHA was launched in January, 1979, into a near-geosynchronous (23 hour, 35-minute), near equatorial orbit with a 7.9 degree inclination. The satellite is cylindrical in shape, spin-stabilized, with a period of rotation of about 58 seconds. The spin axis is in the orbital plane and is maintained normal to the earth-sun line within $\pm$ 5 degrees. The satellite orbit has apogee of 7.8 R_E (earth radii) and perigee of 5.3 R_E. During the spring and fall the satellite enters an eclipse season, a period in which a portion of each orbit intersects the earth's shadow. The maximum eclipse duration per orbit is 71 minutes.

The SC4-2 instrument on the SCATHA satellite was developed to eject currents of positive and negative charge either separately or together. The major elements of the system are a xenon gas storage reservoir, a feed line from the reservoir to a hollow cathode, a discharge chamber, ion optics, a filament neutralizer, and supporting electronics. A functional block diagram of the SC4-2 payload is shown in Figure 1. On command, gas from the reservoir is fed through the hollow cathode and into the discharge chamber. Ions are produced in the discharge chamber by the impact of electrons from the heated cathode with neutral xenon atoms. The ion energy is determined by both the anode-cathode potential difference and the chamber (screen) potential

relative to spacecraft ground. The ions could be ejected from the SC4-2 with low (eV), as well as high (keV), energies. The neutralizer could be independently commanded to be heated, biased with respect to spacecraft ground, or both. Wide dynamic-range electrometers permit measurements of the ion current from the beam power supply, the electron current from the neutralizer emission, and the net emitted current.

The SCI instrument on SCATHA includes a very-low-frequency (VLF) wave analyzer capable of taking broadband measurements of electrostatic and electromagnetic emissions from 0-6 kHz. A 100 meter tip-to-tip dipole antenna (SC10) detects the electric field component (E), and an air-core loop detects the magnetic field component (B) of the waves. The SC10 antenna consists of two 50 meter, 1/4 inch diameter antennas extending from the spacecraft. The sensitivity of the electric field receiver is 5 x 10^{-7} V/m $Hz^{1/2}$ at 1.3 kHz. The air-core loop is electrostatically shielded and has an effective area of 575 m^2 at 1.3 kHz. It is constructed of 1530 turns of 36 AWG copper wire on a form 50 cm in diameter. The antenna is boom-mounted two meters from the central portion of the spacecraft. The sensitivity of the magnetic field receiver is 3 x 10^{-6} γ /$Hz^{1/2}$ at 1.3 kHz. Prior to flight laboratory tests were conducted to insure that the instruments were shielded so there would be no internally generated signals detected by the E and B antennas. During periods of SCI operations presented here the wave environment was sampled alternately for periods of 16 seconds duration with the E and B antennas. Data are presented in a frequency versus time format. A grey scale indicates relative intensities at a given time. The maximum amplitude is measured by the detector's automatic gain control (AGC) system four times per second in unequal intervals. The AGC measurements, plotted in field strength versus time, are given with each data sample. In the frequency-time spectrograms information about wave fields more than 20 db below the frequency of maximum amplitude is supressed.

OBSERVATIONS

During the period between 0747:34 and 0801:45 UT on 24 April 1979 the SC4-2 system on SCATHA operated intermittently in the plasma-beam mode. Throughout this period the satellite was at an altitude of ~ 6.7 R_E in the plasma sheet and in the earth's shadow. Figure 2 contains plots of the emitted ion current (top panel) and the satellite frame potential (bottom panel) for the twelve minutes following 0750:10 UT. Note that when the plasma-beam was not operating the satellite potential ranged between -2 and -3 kV. This potential was discharged during four distinct plasma-beam operating modes. The ion and electron current and energy levels connected with the four plasma beam modes are listed in Table 1. Also listed in Table 1 is the range of maximum amplitudes measured by the electric and magnetic antennas during both background and beam operation intervals. These ranges were determined from the gain states of the AGC. Throughout this paper the word "background" denotes waves detected while the discharge system was not operating.

To help distinguish beam-induced EMI effects from background emissions it is useful to consider VLF measurements from the E and B antennas prior to beam turn-on. The bottom portions of Figures 3a and 3b provide examples of the E and B background measurements, respectively. The curves in the top panels of these figures give the AGC levels of maximum signal intensities. These measurements correspond to the darkest portions of the 0-6 kHz spectrograms. They are given in db V and μV/m for E_{max} and db γ and mγ for B_{max}. The background signals consist of narrow bands, approximately 200 Hz in width centered near 0.6 and 1.2 kHz. The signal near 1.2 kHz is

the most intense. The harmonic bands near 1.7 and 2.2 kHz are believed to be artifacts of ground station instrumentation.

Examples of VLF signals as well as E_{max} and B_{max} as measured during each of the four modes of plasma beam emissions, are presented in Figures 4-7. For ease in comparing intensities of fields measured during beam operations with background measurements E_{max} and B_{max} from Figure 3 are plotted, represented by the symbol 0, with the appropriate beam mode (1, 2, 3, 4). Note that AGC measurements taken immediately after the receiver switches to the electric antenna do not provide reliable values of the electric fields. During these intervals the AGC is searching for the appropriate gain state. Often the appropriate state is considerably lower for the electric than the magnetic antenna. This is because the reference voltage is 1.0 V for the electric receiver and only 300 µV for the magnetic receiver. The system is designed such that the receivers center on chorus emissions and permit the detection of waves within ± 30 db of chorus fields.

The mode 1 beam emissions, from 0753:12 to 0754:08 and from 0800:07 to 0801:45, generated the largest amounts of EMI. In this mode ions were emitted with energies of 1 keV and currents between 1.1 and 1.7 mA. Electrons were emitted from a heated filament biased at -10V with respect to the satellite. Figures 4a and 4b contain examples of B and E signals as well as B_{max} and E_{max} measured during mode 1 operations. The magnetic signal consists of a band extending from 0.5 to 5.0 kHz that has maximum intensities near 1.3 and 3.5 kHz. Since the antenna response maximizes at 1.3 kHz, the greater intensity of that signal band near that frequency is partly an artifact of of the system. However, the null in the noise band near 3 kHz implies that the double-banded structure is real. Values of B_{max} range from 40 to 100 mγ and are consistantly stronger than the background emissions. The electric signal contains narrow bands centered near 1, 2 and 3 kHz with E_{max} in the 20 to 100 µV/m range. The bands that appear between seconds 6 through 8 of Figure 4 are harmonics of the background, double band spectrum. In other mode 1 measurements (not shown) even small-scale rising tone features are exactly replicated in each of the bands. These multiple bands sometimes span the entire 0-6 kHz bandwidth of the detector. The values of E_{max} for the multiple bands lie between 100 and 400 µ V/m. Although E_{max} approaches background values during these periods it is, in general, less than the background E_{max}.

In the second plasma-beam mode (0754:08 - 0756:19 UT) ions were again emitted with 1 keV energy but at current strengths that varied between 0.75 and 0.9 mA. Electrons were emitted with the same filament bias of -10 V with currents slightly more than 1.0 mA. Magnetic and electric signals characteristic of mode 2 operations are shown in Figures 5a and c, and 5b and d, respectively. Again the magnetic signal covers the entire 0.5 to 5 kHz band. However, B_{max} which ranges from 10 to 100 mγ may be either less than or greater than background values. Note that the noise level is reduced and the background signal intensified in the second sample, Figure 5c, compared to the first which is taken at the beginning of the mode. The electric signal is consistently weaker than the background level. The stronger values of E_{max} (40 - 200 µV/m) occur when background frequency signals are visible in the spectrogram. The weaker values of E_{max} occur during periods of 0-1 kHz broadband noise. Note the stronger signals in the second sample, Figure 5d, which is taken in the latter portion of the mode operation. The significance of these changes will be discussed below.

The third plasma-beam mode (0756:19 - 0758:09 UT) was characterized by ion currents of 0.04 mA at energies less than 40 eV. The electron current was 0.45 mA with the filament biased at -10 V. VLF data representative of this beam mode are

presented in Figure 6. The magnetic signal appears as a band, decreasing in intensity with increasing frequency, covering the 0.5 to 4 kHz range. The most intense signal is near 1.2 kHz with B_{max} between 10 and 20 mγ. This is lower in intensity than the background signals of Figure 3. Some narrow band signals are barely discernible near 2.8, 3 and 5 kHz between seconds 0 to 2 and 8 to 13. The electric signal is more complex. It includes a persistent narrow band at the background frequency of 1.2 kHz and intermittent signals at 0.6, 2.2 and 5 kHz. Note also the presence of a multiple band near 3 kHz. The portion of this spectrogram between 4 and 6 seconds and 9 and 11 seconds shows that the signal near 2.8 kHz can exceed the 1.2 kHz signal in intensity. These periods are also marked by the presence of narrow bands near 0.1 kHz. Throughout this plasma-beam operation E_{max} was between 40 and 200 μV/m, again less than the intensity of background signals.

The fourth beam mode started at 0759:10 UT as a discharge in the ion source chamber that lasted until 0800:07 UT. The current electrometer measured a net <u>positive</u> current of 0.01 mA. The energy of the ejected positive charge was < 40 eV. During this interval the satellite frame discharged from -2.7 kV to within 100 V of plasma potential. Corresponding B and E signals are presented in Figure 7. The magnetic signal appears as a band of variable intensity, from 0.5 to 5 kHz, with B_{max} in the 10-30 mγ range near 1.2 kHz. This is similiar to but stronger in intensity than signals detected during mode 3 operations. A comparison of AGC levels with the spectrogram shows that in mode 4 B_{max} is usually less than the background level. Narrow-band signals near 5 kHz are visible when B_{max} is weakest. The electric signals also have characteristics similiar to those of mode 3 operations. The mode 4 electric signals, however, contain numerous bursts that cross the entire band. E_{max} varies betwen 40 and 200 μV/m. The background signal at 1.2 kHz was dominant during periods of strongest signals. During periods of weaker signals (seconds 5 to 7 and 12.5 to 14.5) the 0.6 kHz band and 0 to .5 kHz noise was dominant.

SUMMARY AND DISCUSSION

To provide a context for interpreting the VLF measurements presented above it is useful to summarize the plasma and magnetic field environment of SCATHA. During the period of interest the SCATHA dc magnetometer measured magnetic fields in the 75-80 nT range. Thus, the electron gyrofrequency, f_e, was ~ 2 kHz. There were no measurements of the cold plasma (< 10 eV) by SCATHA Instruments. The Rapid Scan Particle Detector (SC5) measurements of electrons and ions with energies between 50 eV and 1 MeV have been discussed in reference 7. During the period of spacecraft charging the density of plasma sheet electrons in the energy range of detectability was between 0.5 and 1 cm^{-3}. Corresponding plasma frequencies and upper hybrid frequencies, which lie in the 6.3 to 10 kHz range, cannot be detected by the SCATHA VLF receiver. It is interesting to note that the charging period corresponded to an injection of high energy (30 - 335 keV) electrons whose combined fluxes strongly correlated with the satellite potential. Electrons in this energy range were highly anisotropic with maximum fluxes perpendicular to the magnetic field.

The background signals shown in Figure 3 consist of a double band that appears in both the electric and magnetic field spectrograms. Thus, they are electromagnetic rather than electrostatic phenomena. The frequencies are centered at 0.6 and 1.1 kHz with a null near 0.5 f_e. There is a weaker double band with a similiar structure with frequencies centered at 1.7 and 2.2 kHz and a null near f_e that is considered to be an artifact of the ground station instrumentation.

397

The double-banded electromagnetic emissions with a null near 0.5 f_e are a form of magnetospheric chorus that has been discussed extensively in the literature (refs. 8-14). There is general agreement that chorus emissions result from a Doppler-shifted, cyclotron resonance between anisotropically distributed, energetic electrons and generally present background, electromagnetic noise. The energy of resonant electrons, derived in reference 4, is:

$$E_R = \frac{B^2}{8\pi n} \left(\frac{f_e}{f}\right) \left(1 - \frac{f}{f_e}\right)^3$$

With the observed magnetic field 75-80 nT and electron densities 0.5 - 1.0 cm^{-3} the magnetic energy density per particle lies between 14 and 32 keV. Setting $f = .5 f_e$ we estimate a band of resonant energies extending from 3.5 to 8 keV. Electron measurements from this period reported in reference 7, show that anisotropic electrons in this energy range were present in abundance. To the best of our knowledge, there is no generally accepted explanation for the missing emission band near 0.5 f_e.

Examples of the effects of plasma beam emissions on the detection of electric and magnetic signals at VLF frequencies have been presented in Figures 4-7. Before the plasma beams were ejected, between beam emissions and after beam turn-off, the vehicle was charged several kilovolts and discrete, narrow-band emissions were detected by the electric and magnetic receivers. As shown in Table 1 the values of E_{max} and B_{max}, with no beam emissions were in the ranges 200-600 μV/m and 20-60 mγ, respectively. To varying degrees the detection of background electric and magnetic VLF signals was compromised during four distinct modes of plasma-beam operations that discharged the satellite. During beam operations magnetic spectrograms were characterized by broad bands extending from 0.5 to 5 kHz that make visual identification of background signals difficult. The intensity of B_{max} varied with the strength and duration of the emitted current. The electric field spectrograms more readily provide information about background signals. The narrowband, background signal near 1.2 kHz is nearly always present. However, there are electric field signals at other than "background" frequencies. The AGC measurements, summarized in Table 1 show that E_{max} was consistently lower with the beam on than during beam-off periods.

Before considering the wave measurements during beam operations, it is useful to attempt a description of the zero-order effects of the plasma beam in the immediate vicinity of the satellite and the VLF sensors. There is evidence from the active potential control experiments on ATS-5, ATS-6 and SCATHA that plasma beams are successful in discharging differentially charged surfaces as well as the conducting frame of the satellite (refs. 6 and 15). From an analysis of SCATHA experimental data, in reference 15 it is shown that different physical processes must be responsible in each case. To begin with, the plasma beam must be dispersed such that a cloud eventually envelopes the whole satellite. To discharge the negatively charged satellite frame most beam electrons must escape to infinity. The discharge of dielectric surfaces requires that positive ions from the emitted beam impact these surfaces in sufficient numbers to neutralize negative charges deposited from the magnetospheric plasma. Secondary electrons from the impacting beam ions and magnetospheric electrons probably play crucial roles in this discharging procedure. Whatever the details of the discharging process may be, two things are clearly required. First, the sheath in the immediate vicinity of the satellite is transformed from a depleted plasma to an enhanced plasma. The extent of the enhancement sheath is not known. Second, the near satellite enhancement

region is characterized by multiple, complex current loops that couple dielectric surfaces with the magnetospheric plasma and the satellite frame. Recall that the air core loop is located 2 m from the satellite while the active element of the electric field antenna extends from 20 to 50 m from the satellite. If the scale size of the plasma-enhanced region is less than 50 m very different effects on the two systems may be anticipated.

The magnetic spectrograms are dominated by wide bands that extend from 0.5 to 5 kHz. The apparent low frequency cut off is an instrumental effect. At frequencies less than 1 kHz the frequency response of the magnetic VLF receiver decreases rapidly with decreasing frequency (cf Figure 2 of ref. 14). The presence of an enhanced plasma in the immediate vicinity of the satellite should of itself, have no effect on the performance of the low impedance loop antenna (ref. 16). Rather, the data suggest that the air core loop is embedded in a dense region of fluctuating currents inherent to the satellite discharge process. These bands may have harmonic structure (figures 4a and 5a) with intensity exceeding that of the background signals. The signal strength intensifies just below the first and second harmonics of the electron gyrofrequency; i.e., 2 kHz and 4 kHz, respectively. One possible explanation comes from Ohnuma, et al., (ref. 17). They have shown that in a high density, hot plasma, electromagnetic waves may be generated at these harmonics. These waves are back-scattered at some critical low density which implies they would be confined to the enhanced sheath region around the satellite.

Structured emissions are detectable, to varying degrees during all beam operations but are more easily perceived in the electric field spectrograms. These emissions have five different kinds of signatures: (1) chorus emissions centered at .6, and 1.2 kHz, (2) chorus harmonic bands,(3) narrow bands near 3 and 5 kHz, (4) multiple bands near 3 kHz, and (5) 0 to .5 kHz ELF bands. The background chorus signals centered at 1.1 kHz were present a large fraction of the time while those at 0.6 kHz were less frequently detectable. Intensities of chorus signals were usually well below those measured when the beam system was off. The diminished and sometimes totally suppressed chorus seems to be related to the beam emission process rather than to variations in the emitting plasma. This is evidenced by the relative constancy of (1) E_{max} and B_{max} when the beam was off and (2) the flux levels and pitch angle distributions of electrons in the resonant energy range of 5 to 10 keV. A possible mechanism for reducing chorus intensity measurements is discussed below.

Multiple harmonics of chorus emissions are occasionally detected during mode 1 operations, and are most visible on the electric field spectrograms (figure 4b). The fact that multiple harmonics only appear during a specific mode of operation and have never been detected outside beam operations suggests that they are artifacts of the beam emission process. How they are produced is not understood at this time. It may be that the beam emission which is highly anisotropic occurring at pitch angles of 70°-140°, or the vehicle discharging process, create sufficiently energetic, anisotropic electrons to produce cyclotron harmonic resonances as discussed in references 4 and 18, which in turn may produce harmonics of chorus emissions. In the near vicinity of the satellite, the high current emissions are shown to intensify the 1.2 kHz signal (figures 4a and 5a).

At sometime during all four modes of plasm-beam operations narrow bands near 3 kHz are visible in the spectrograms. A similar band at 5 kHz is detectable intermittantly during modes 3 and 4. These signals are present in both the electric and magnetic spectrograms. They appear to be electron cyclotron harmonic (ECH) waves. Wave modes of these types propagate nearly perpendicular to the magnetic field between harmonics of the electron gyrofrequency and may be associated

with positive slopes in the electron distribution function ($\partial f/\partial v_\perp > 0$).
However, the responsible electrons have energies considerably lower than those responsible
for chorus waves (ref. 2). We note that on several occasions the appearance
of ECH waves coincided with the complete suppression of the 1.2 kHz chorus band.

The observation of a magnetic component is contrary to other observations in
space (ref. 3) and is not yet understood. The ECH waves are assumed to have
long wavelengths, much greater than the 50 cm diameter of the magnetic loop antenna.
Therefore, there should be no coupling of the wave electric fields to this antenna.
It may be, however, that these waves generate local current oscillations in the
satellite sheath in which the magnetic antenna is imbedded. These oscillations
would occur at the same frequency as those of the naturally occurring ECH waves.

During the entire mode 3 and seconds 11 to 16 of mode 4, multiple bands are
detected near 3/2 f_e. Similar multiple bands have been reported by Koons and
Fennell, (ref. 20). They are usually associated with electrons at energies of a
few keV whose distribution functions have relative minima at pitch angles of 90°.
We have examined particle measurements and found that at the times of modes 3 and
4, electrons with energies of ~ 1 keV had trapped pitch angle distributions but
with a local minimum at 90°. Electrons in all other energy channels have normally
trapped distributions.

Sporadic emissions of signals in the 0 to .5 kHz range were detected during
all four beam modes on the electric field spectrograms. Similar ELF bursts have
been detected (ref. private communication, 1982) during beam-off periods. Again we
note that several of these bursts (Figures 5 and 7) coincide with periods in which
the 1.2 kHz signal is completely suppressed.

Since the ECH and ELF emissions naturally occur in plasma sheet environments
this is probably true in the present case as well. Their appearances during beam
operations frequently coincide with low amplitudes or absences in the chorus bands.
This suggests that when the beam system is not operating the ECH and ELF waves are
more than 20 db below background chorus intensities. Only when the level of detected
chorus signals is diminished or supressed does the AGC react to the presence of
these waves. The question of beam related EMI thus becomes, how does the beam emission
process lead to diminished chorus measurements by the antenna systems. Two possible
mechanisms come to mind: (1) diminshed antenna coupling between the antenna and the
medium, and (2) interactions between the chorus and the plasma cloud around the
satellite.

The first alternative, diminished antenna coupling with the medium applies only
to the electric antenna and does not seem to be correct for two reasons. First,
during beam emission periods the density of particles in the sheath around the antenna
should be increased. This leads to a decreased sheath impedance (ref. 16) and
better coupling to the medium (ref. 21). Second, there is no reason for the antenna
to be coupled efficiently to the medium at 0.0 to 0.5 kHz and at 3 kHz and inefficiently
coupled at 1.2 kHz.

The vehicle discharging process results in the emission of secondary electrons
from dielectric surfaces. In reference 15 it is shown that these surfaces discharge
at different rates based on surface material and location. Independent of material,
a surface which was readily accessible to beam ions would discharge more rapidly
than one that was in a less accessible location on the satellite. The discharging
of the satellite frame was almost instantaneous whereas the rate for each sample
varied such that discharging occurred over a period on the order of minutes. This

indicates that secondary electrons are emitted over this entire period with varied and decreasing energies depending on the particular surface from which they were emitted, its location and rate of discharge. These electrons would produce a cloud of varied length and diameter that decreased in time. This is indicated by comparing the two samples of mode 2. The first sample shows considerable suppression of the background signal on the E and B spectrograms even with a reduced noise level on the B spectrogram. The second sample indicates a greater variability in the plasma cloud permitting more of the background signal to penetrate on the E spectrogram and intensification of the 1.2 kHz signal on the B spectrogram.

The direction of wave propagation for chorus and ECH waves combined with an assymetry of the local plasma could could lead to a selective diminution of chorus. Chorus waves usually propagate in directions close to that of the magnetic field while ECH waves propagate mostly normal to the magnetic field. Because particles in the plasma cloud emitted during beam operations are relatively free to move along but not across the magnetic field the cloud could have a relatively large extent along the magnetic field. Waves propagating along the magnetic field could see an "optically thick" medium while those propagating across the magnetic field an "optically thin" medium.

Chorus waves amplify due to the presence of free energy contained in the anisotropic pitch angle distributions of resonant, energetic electrons. They are also subject to Landau damping processes. Waves grow in regions where the free energy available exceeds the rate at which Landau heating of the plasma occurs. The introduction of large quantities of low-energy electrons in the plasma cloud greatly increases the negative slope of the total electron distribution function and consequently the rate of Landau damping. The length and diameter of the plasma cloud along the magnetic field would then modulate the admittance of chorus waves to the satellite. The diameter of the cloud should be limited to a few electron gyroradii. For emitted 10 eV electrons this is of the order of a few hundred meters; for 2-3 keV secondary electrons this is of the order of kilometers. Since the Debye length in the plasma sheet is several kilometers such a cloud should have little effect on perpendicularly propagating waves.

CONCLUSIONS

The combination of plasma beam emissions and the discharging process has been shown to have three distinct affects on the detection of VLF waves. First, the magnetic loop antenna detects intense signals during high current emissions, modes 1 and 2, that are apparently localized to the near vicinity of the satellite. They are assumed to be generated and/or amplified within the plasma that envelopes the satellite upon beam emission. These signals span the 0.5 to 5 kHz band, may be double-banded, and often saturate the magnetic receiver, thus obscuring the detection of signals that do not lie within 20 dB of this signal amplitude. Second, on the electric antenna during mode 1, the highest current emitting mode, occasionally multiple bands of chorus emissions are detected. These are assumed to be generated by the large anisotropic fluxes of beam electrons. Third, the fields of the chorus emissions are often suppressed. This suppression permits observations of much weaker wave fields. It is suggested that electrons emitted by the beam and during the discharge process create an irregular plasma cloud along the field lines which becomes an optically thick screen for parallel propagating waves.

REFERENCES

1. Garrett, H.B., The charging of spacecraft surfaces, Rev. Geophys and Sp. Phys., 19, 577, 1981.

2. Young, T.S.T., Electrostatic waves at half electron gyrofrequency, J. Geophys. Res., 79, 1985, 1974.,

3. Ashour-Abdalla, M. and R.M. Thorne, Towards a unified view of diffuse auroral precipitation, J. Geophys. Res., 83, 4755, 1978.

4. Kennel, C.F. and H.E. Petschek, Limit on stably trapped particle fluxes, J. Geophys. Res., 71, 1, 1966.

5. Lyons, L.R. Electron diffusion driven by magnetospheric electrostatic waves, J. Geophys. Res., 79, 575, 1974.

6. Purvis, C.K., and R.O. Bartlett, Active control of spacecraft charging, in Space Systems and Their Interactions with Earth's Space Environment, Prog. Astronaut. Aeronaut., vol. 71, edited by H.B. Garrett and C.D. Pike, pp. 299-317, American Institute of Aeronautics and Astronautics, New York, 1980.

7. Gussenhoven, M.S. and E.G. Mullen, Geosynchronous environment for severe spacecraft charging, J. Spacecraft and Rockets, 20, 26, 1983.

8. Burtis, W.J. and R.A. Helliwell, Banded chorus--A new type of VLF radiation observed in the magnetosphere by OGO 1 and OGO 3, J. Geophys. Res., 74, 3002, 1969.

9. Burton, R.K., C.T. Russell, and C.R. Chappell, The Alfven velocity in the magnetosphere and its relationship to ELF emissions, J. Geophys. Res., 75, 5582, 1970.

10. Burton, R.K., and R.E. Holzer, the origin and propagation of chorus in the outer magnetosphere, J. Geophys. Res., 79, 1014, 1974.

11. Tsurutani, B.T. and E.J. Smith, Postmidnight chorus: a substorm phenomenon, J. Geophys. Res., 79, 118, 1974.

12. Tsurutani, B.T. and E.J. Smith, Two types of ELF chorus and their substorm dependences, J. Geophys. Res., 82, 5112, 1977.

13. Anderson, R.R., and K. Maeda, VLF emissions associated with enhanced magnetospheric electrons, J. Geophys. Res., 82, 135, 1977.

14. Koons, H.C. and J.F. Fennell, Fine structure in electrostatic emission bands between electron gyrofrequency harmonics, EOS, 63, 1074, 1982.

15. Cohen, H.C. and S.T. Lai, Discharging the P78-2 satellite using ions and electrons, Proceedings of AIAA 13th Aerospace Science Conference, Orlando, Florida, January, 1982.

16. Koons, H.C. D.A. McPherson, and W.R. Harbridge, Dependence of Very-Low Frequency electric field antenna impedance on magnetopheric plasma density, J. Geophys. Res., 75, 2490, 1970.

17. Ohnuma, T. and T. Watanabe, Wave fronts of electromagnetic cyclotron harmonic waves, Phys. Fluids, 25, 1217, 1982.

18. Lyons, L.R., R.M. Thorne and C.F. Kennel, Pitch-angle diffusion of radiation belt electrons within the plasmaphere, J. Geophys. Res., 77, 3455, 1972.

19. Young, T.S.T., J.D. Cullen and J.E. McCune, High frequency electrostatic waves in the magnetosphere, J. Geophys. Res., 78, 1082, 1973.

20. Koons, H.C., The role of hiss in magnetospheric chorus emissions, J. Geophys. Res., 86, 6745, 1981.

21. Fahleson, U., Theory of electric field measurements conducted in the magnetosphere with electric probles, Space Sci. Rev., 7, 238, 1967.

TABLE I. – CONDITIONS DURING PLASMA BEAM MODES

Plasma Mode	Ion Current (mA)	Ion Energy (keV)	Electron Current (mA)	Electron Energy (keV)	Maximum Field Strength	
					Electric (kv/m)	Magnetic (m ,)
0	0	0	0	0	200-600	20-60
1	1.1 - 1.7	1.0	2.1 - 2.4	0.01	20-400	40-10
2	0.75 - 0.9	1.0	1.0	0.01	10-200	20-10
3	0.04	0.04	0.45	0.01	40-200	10-20
4	0.01	0.04	0.0	0.0	40-200	10-20
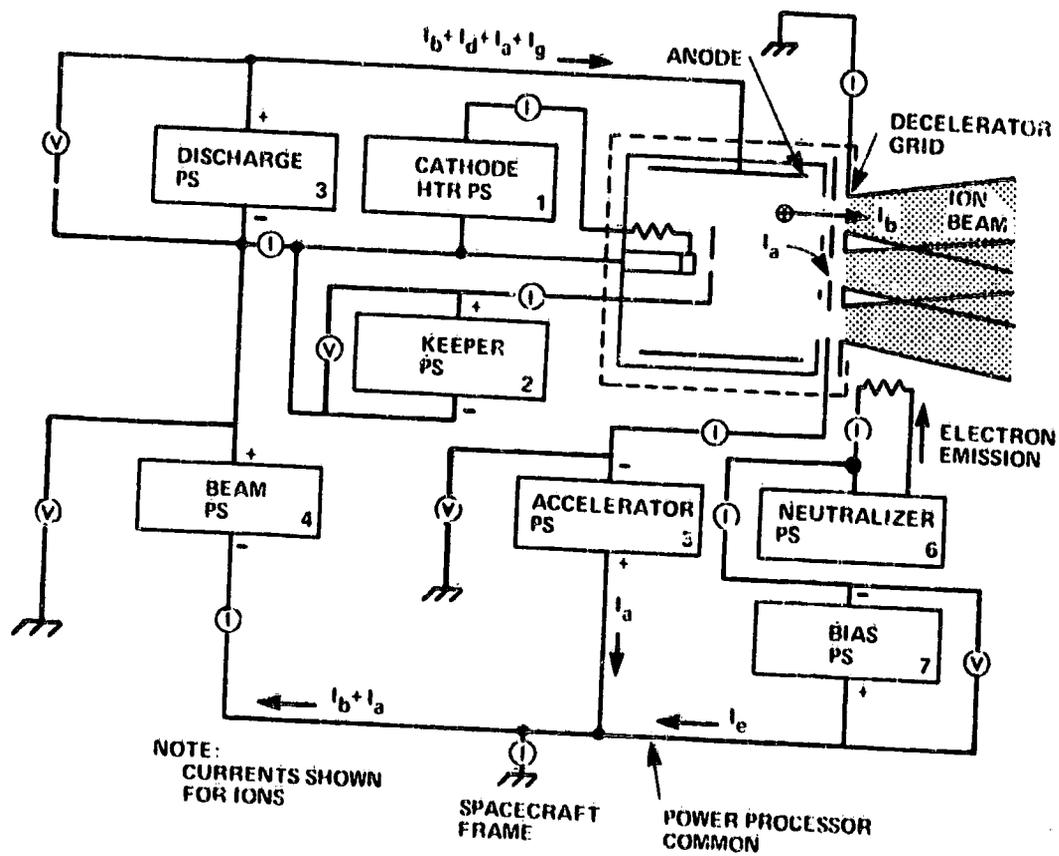
Figure 1. – Functional block diagram of ion source and power processor for SC-4.
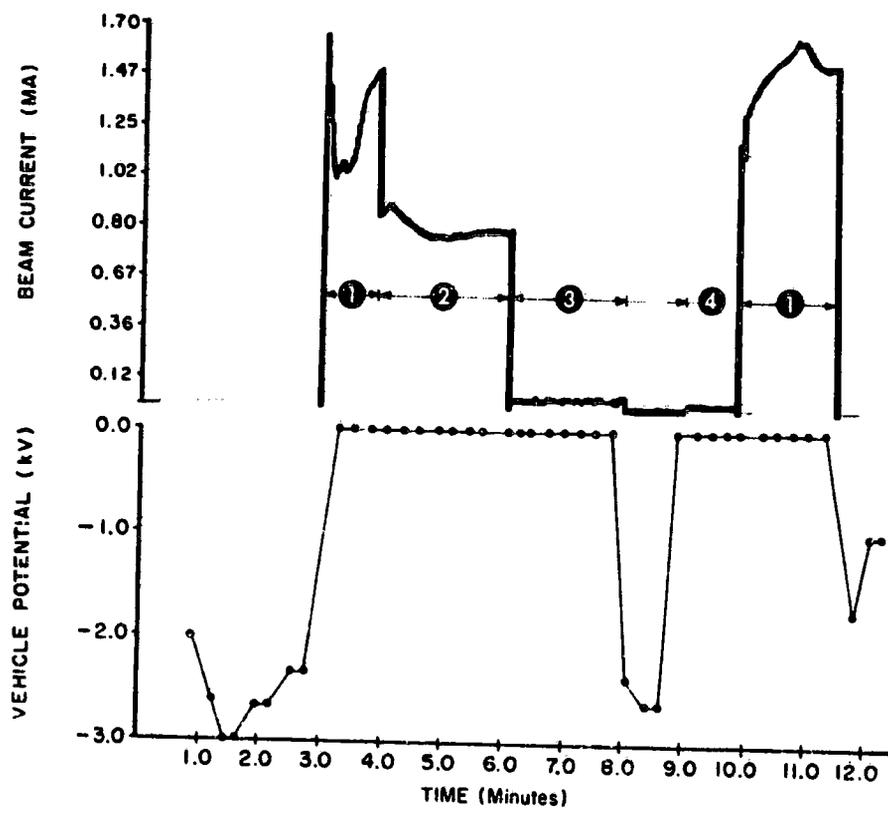
Figure 2. – Ion beam current and vehicle potential during the four modes of plasma beam operations. (Note the response of the vehicle potential to the beam emission.) T_0 = 07:50:10.

Figure 3. – Background wave fields detected by VLF broadband receiver. (Relative intensity of wave fields is indicated by grey scale with darkest being most intense portion. In this case it is chorus band just above 1 kHz. This intensity is plotted above recorded field signals as 0-curve, given in dBγ and mγ for magnetic field and dBV and μV/m for electric field.)
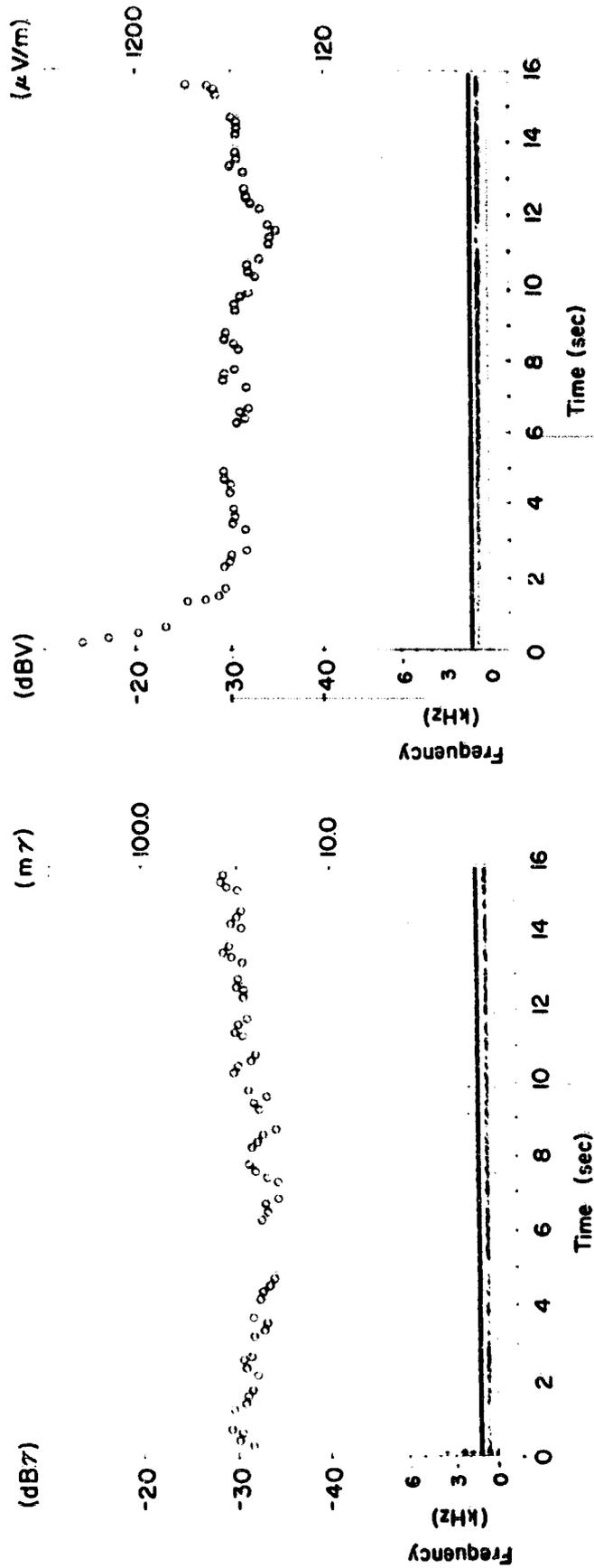
(a) Magnetic loop antenna. T_0 = 07:46:27.75.

(b) Electric dipole antenna. T_0 = 07:46:11.75.

(μV/m)

- 1200

- 120

- 12.0

(dBV)

-20

-30

-40

-50

-60

Frequency
(kHz)

6
3
0

0 2 4 6 8 10 12 14 16

Time (sec)

(b) Electric dipole antenna. $T_0 = 08:00:35.75$.

Figure 4. - Signals detected during mode 1 plasma beam operations with ion beam current of 1.1 to 1.7 mA. (The curve of maximum background field intensity from fig. 3 (0-curve) is replotted here for comparison with signal intensity during beam operations (1-curve). Note the double-banded structure of the magnetic field signal band and the complex multiband structures in the electric field signal that vary with maximum field intensity.)

(mγ)

- 100.0

- 10.0

- 1.0

(dBγ)

-20

-30

-40

-50

-60

Frequency
(kHz)

6
3
0

0 2 4 6 8 10 12 14 16

Time (sec)

(a) Magnetic loop antenna. $T_0 = 08:00:19.75$.

Figure 5. – Signals detected during mode 2 plasma beam operations with ion current of 0.7 to 0.9 mA. (Double-banded structure is still apparent in magnetic field data.) Electric field data are less structured although maximum field intensity (2-curve) is still quite variable.)
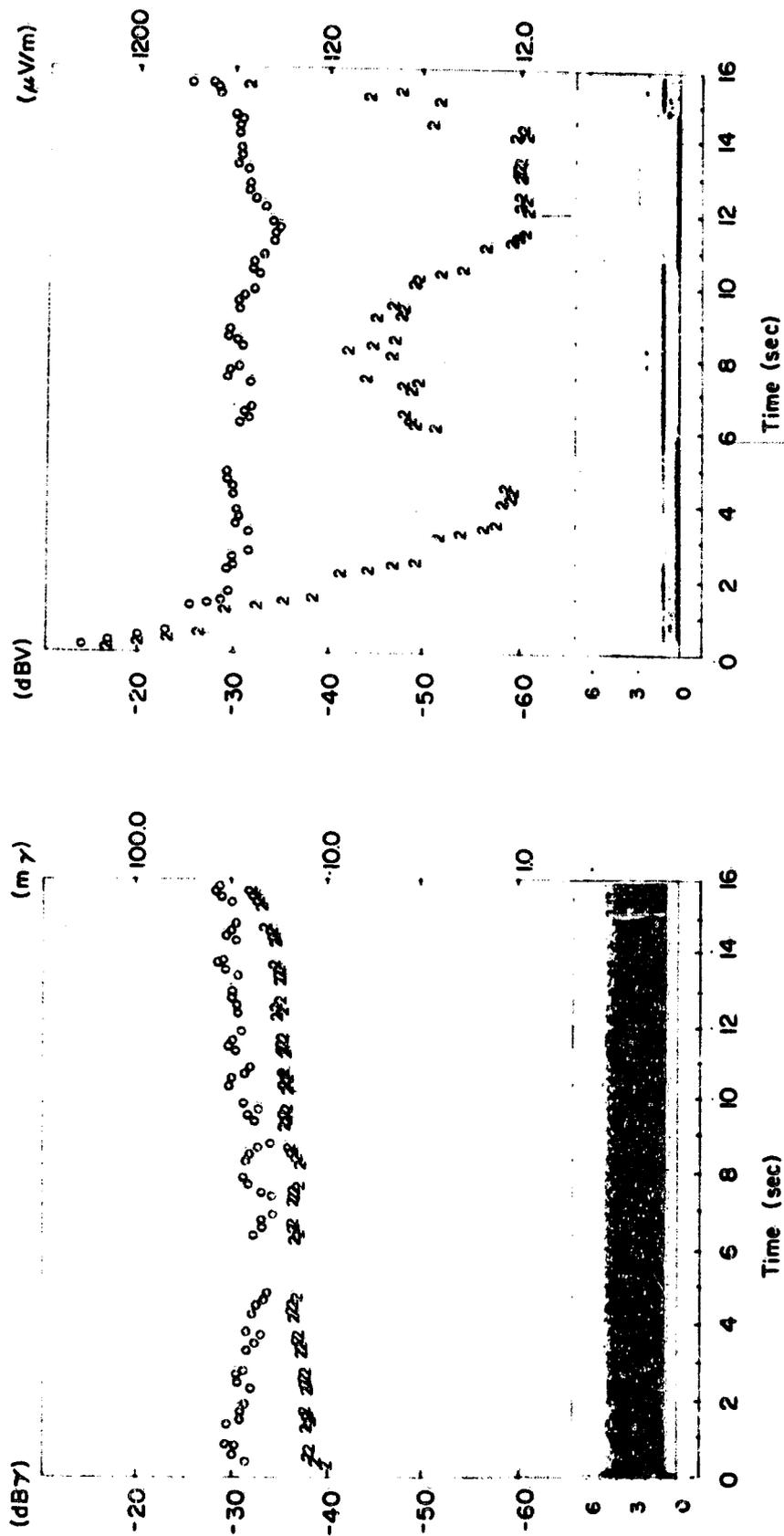
(a) Magnetic loop antenna. $T_0 = 07:54:27.75$.
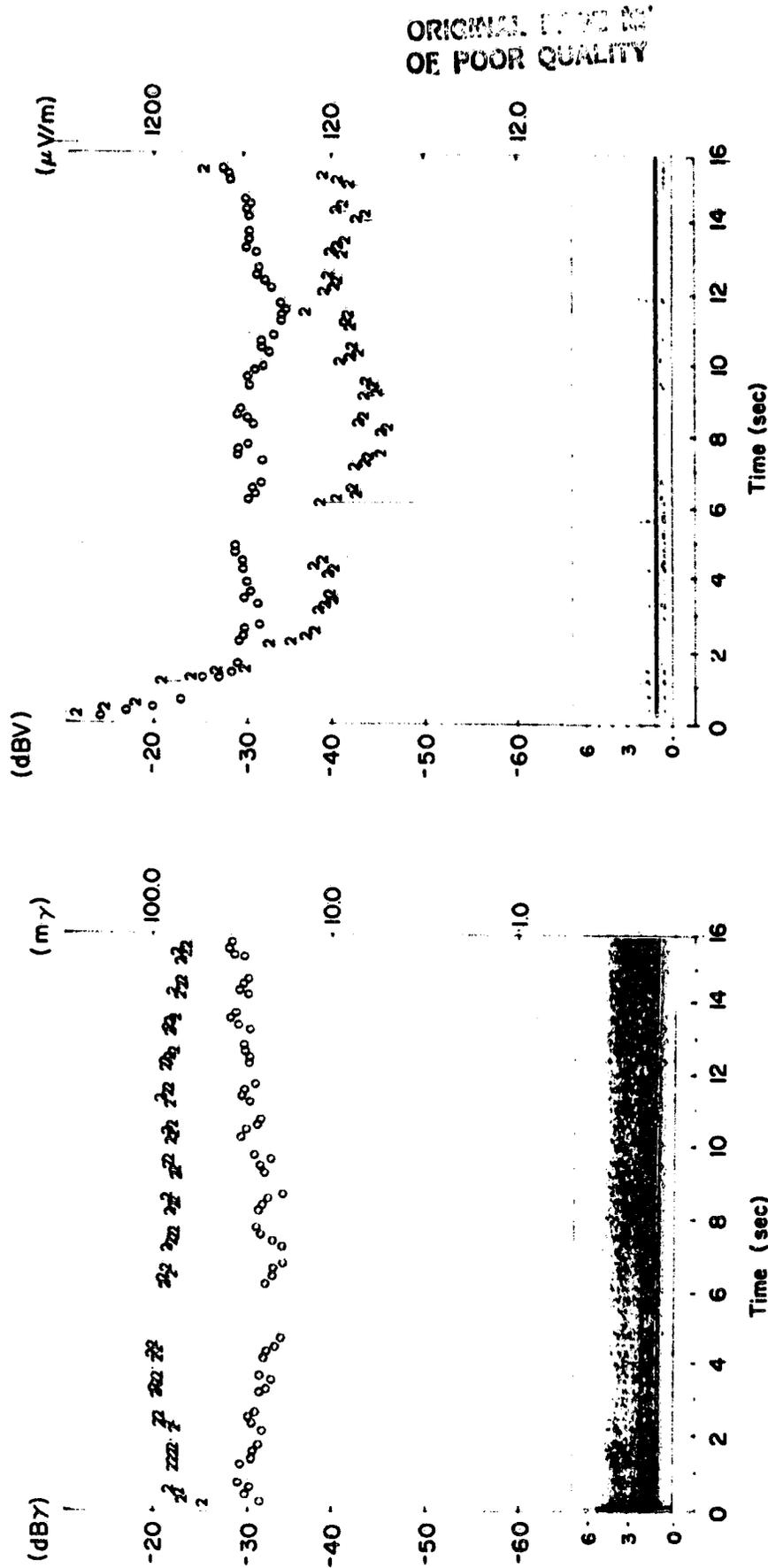
(b) Electric dipole antenna. $T_0 = 07:54:43.75$.

(a) Magnetic loop antenna. T_0 = 07:55:31.75.

(b) Electric dipole antenna. T_0 = 07:55:47.75.

Figure 5. - Concluded. (Here change in signal with duration of plasma beam emission is apparent. Both electric and magnetic field signals are stronger and more nearly resemble background structure of fig. 3, although signal strengths (2-curves) are quite different.)

Figure 7. - Signals detected during mode 4 plasma beam operations with ion beam current of about 10 μA. (Maximum signal intensity (4-curve) is variable in both fields as is signal structure.)
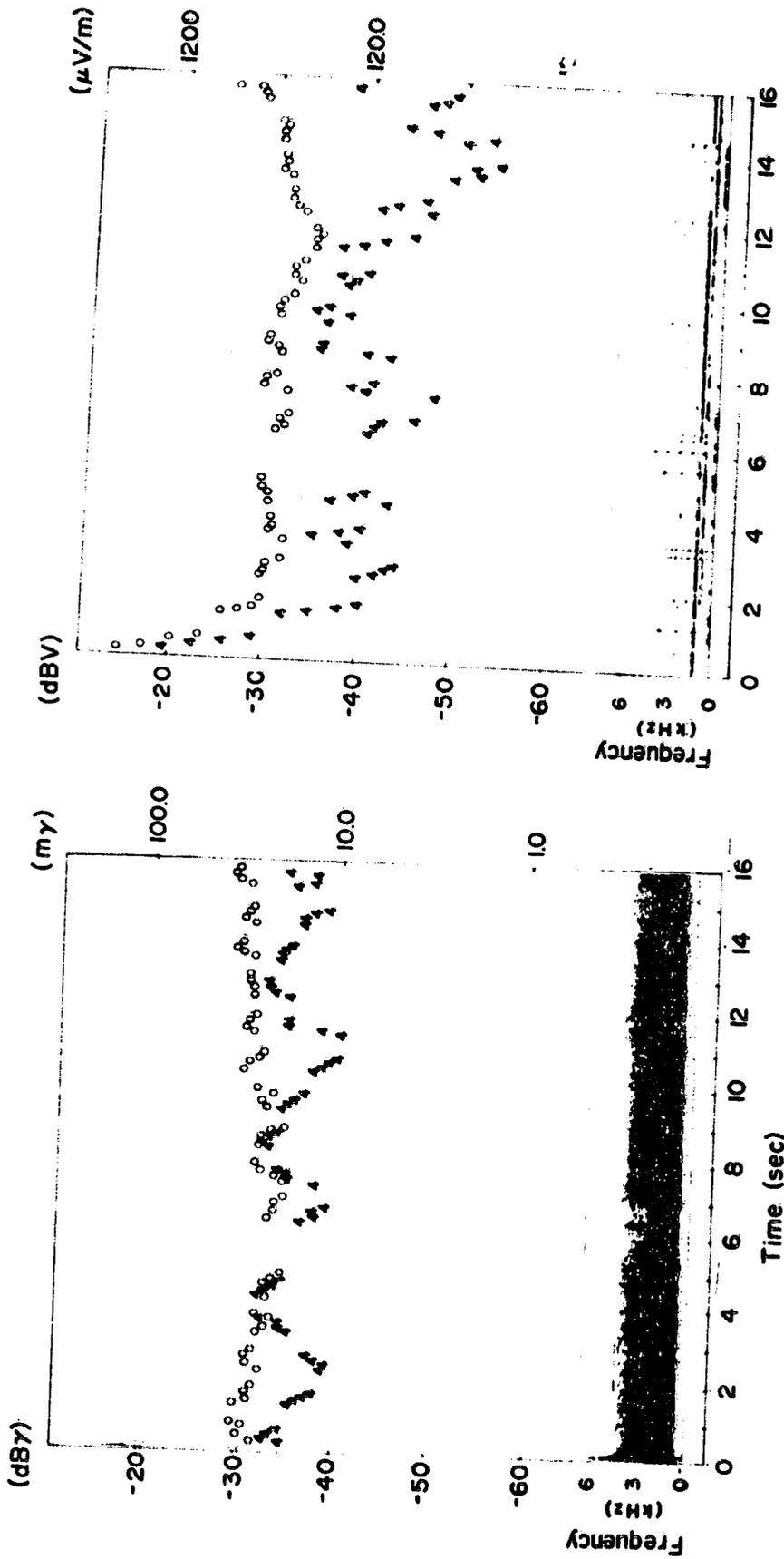
(a) Magnetic loop antenna. T_0 = 07:59:15.75.

(b) Electric dipole antenna. T_0 = 07:59:31.15.

410

(μV/m)

1200

120.0

12.0

(dBV)

−20

−30

−40

−50

−60

Frequency (kHz)

6   3   0

0   2   4   6   8   10   12   14   16

Time (sec)

(b) Electric dipole antenna. T_0 = 07:56:51.75.

(mγ)

100.0

10.0

1.0

(dBγ)

−20

−30

−40

−50

−60

Frequency (kHz)

6   3   0

0   2   4   6   8   10   12   14   16

Time (sec)
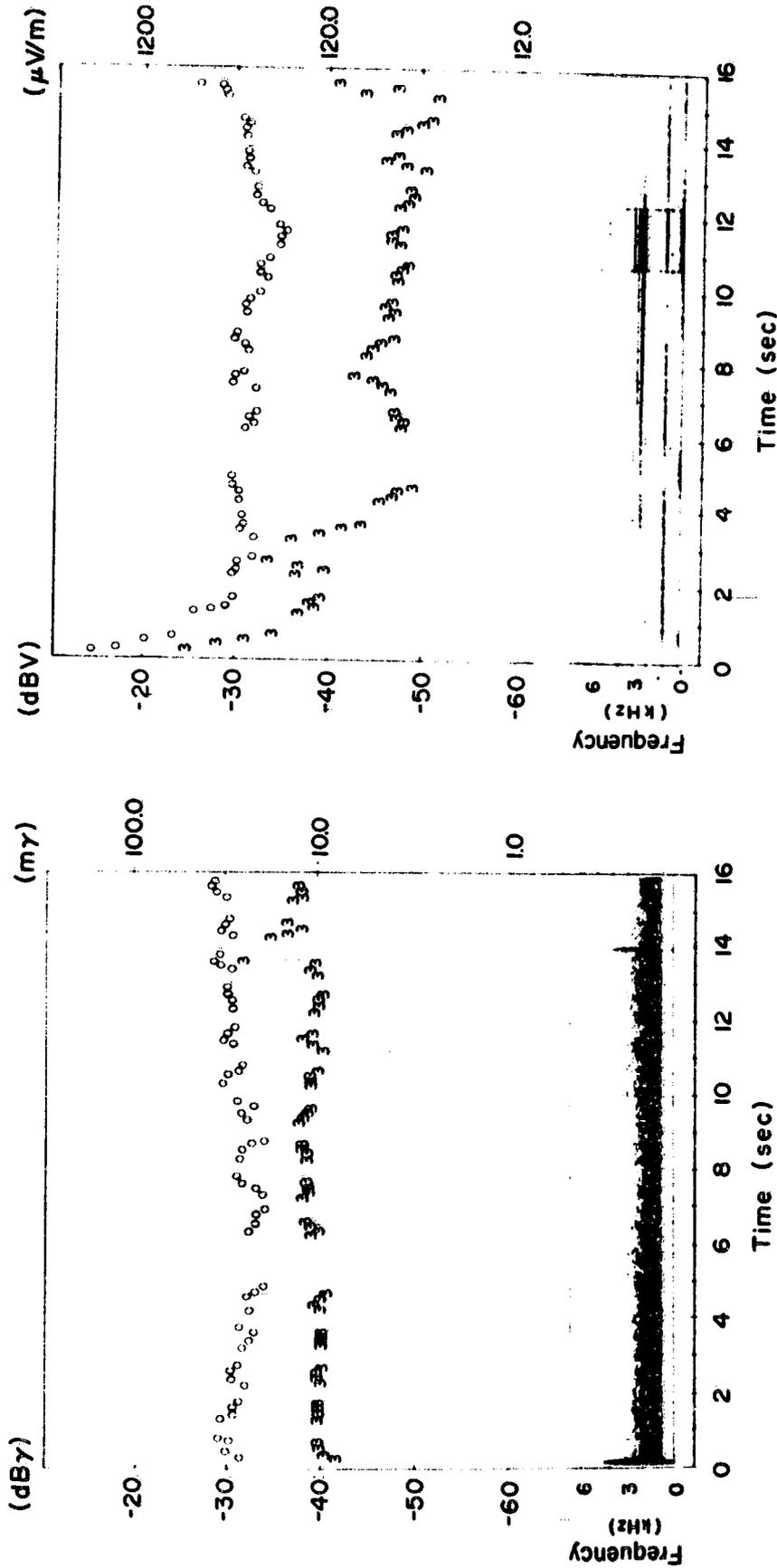
(a) Magnetic loop antenna. T_0 = 07:57:07.75.

Figure 6. – Signals detected during mode 3 plasma beam operations with ion
beam current of about 40 μA. (Both magnetic and electric field signals are
weak. Traces of signal bands are just barely visible in magnetic field data;
electric field data are quite structured.)

411